Study on optical characteristics of wideband anti-reflective enhancement based on silicon square nanoconical hole arrays

KEXIANG HU[a,c*], PEIHUA WANGYANG[b], LE CHEN[c], QINGKANG WANG[c]

[a]*National and Local Joint Engineering Laboratory of Internet Technology on Mine, School of Information and Control Engineering, China University of Mining and Technology, 1 Jinshan East Road, Quanshan District, Xuzhou 221008, P. R. China*

[b]*Sichuan Province Key Laboratory of Information Materials and Devices Application, College of Optoelectronic Technology, Chengdu University of Information Technology, Chengdu 610225, P. R. China*

[c]*National Key Laboratory of Micro/Nano Fabrication Technology, Key Laboratory for Thin Film and Microfabrication Technology of Ministry of Education, School of electronic information and electrical engineering, Shanghai Jiao Tong University, 800 Dongchuan Road, Minhang District, Shanghai 200240, P. R. China.*

In this paper, the optical properties and the electromagnetic field energy density distribution of the silicon square nanoconical hole (SiSNH) arrays are systematically studied via simulation based on Rigorous Coupled Wave Analysis (RCWA) and Finite Difference Time Domain (FDTD). The results show that when the SiSNH top diameter (D_{top}) equal to the array periodicity, the high-efficiency solar energy harvesting will be obtained. When the SiSNH's D_{top} equals to the array periodicity (700 nm), the bottom diameter (D_{bot}) equals to 100 nm and the array length reaches 1800 nm (which contains the hole depth of 1000 nm and the film thickness of 800 nm), the geometrical parameters of the light trapping structure are optimized well and the broadband optical absorption could be enhanced. The optimized SiSNH surface textured crystalline silicon thin film solar cell could yield an ultimate photoelectric conversion efficiency of 38.48%, which is 2.78 times of a 2.33 μm thick film solar cells. Comparing to nanopillar and square nanoconical frustum structures (SiSNF), the photoelectric conversion efficiency of SiSNH surface textured crystalline silicon thin film solar cell is less sensitive to the SiSNH's D_{bot}. In addition, energy density distribution of the light field in the optimized light trapping array above and the physical mechanism behind the observation are also explored in this work.

(Received September 25, 2016; accepted August 9, 2017)

Keywords: Light trapping, Energy density, Photoelectric conversion, Guided-mode resonance

1. Introduction

In the global energy consumption increasing situation, due to the abundant and green source, nearly ideal band gap and the mature processing technology, the bulk silicon material are still dominating the solar cells market. However, the bulk silicon (100 μm or thicker) solar cells require expensive manufacturing process such as purification and crystallization to collect photo-generated carriers efficiently [1]. Recently, many researchers have focused on surface nanotextured silicon film solar cells [2-8] for addressing the issue of photocarrier. Comparing with the conventional bulk Si solar cells, surface nanostructure on Si film solar cells not only could reduce the silicon materials consumption, but also be compatible with the integrated-circuit fabrication techniques. Especially, silicon nanostructure plays an important role in respect of light trapping and carrier collection decoupling via radial p-n junction, thus this will lead to reduction of carrier collection length [9-13], and the silicon material which have properties of the low purity and the short diffusion length could also achieve high power conversion efficiency. There are some theoretical and experimental work in respect of nanopillar [2] and nanohole [8] arrays. Consequently, high aspect-ratio surface nanotexture with an excellent light trapping capability needs to develop urgently for manufacturing high-efficiency and low-cost Si thin film solar cells.

Recently, Li and Yu have demonstrated that hemisphere arrays, hemispherical nanopit arrays and nanocone arrays surface texturing with low aspect ratio have excellent optical properties for photovoltaic applications [3-6]. Zhang and coworkers have analyzed the physical mechanism of nanocone grating surface texturing based on solar cells, especially analyzed the absorption enhancement in the visible wavelength range [7]. Wang and

Leu have systematically simulated optical properties of silicon square nanoconical frustum arrays, their results show that square nanoconical frustum arrays have significantly improved solar absorption and photoelectric conversion, and the enhanced efficiency is insensitive to the top diameter [14]. Guo et al. have carefully studied the advanced light-trapping effect of silicon solar cells with nanocone arrays, nanowires and the tapered nanoholes arrays, and they have also obtained the better antireflective performance and the higher ultimate conversion efficiency [15-18]. In addition, there are also a lot of manufacture works on silicon hexagonal nanoconical frustum arrays, which also have low aspect ratio as well as the advantage of easy fabrication via Langmuir-Blodgett assembly and etching [18-22]. Especially, Chen and coworkers have enhanced the conversion efficiency by 33% via combining the c-Si hexagonal nanoconical frustum arrays solar cells with CdS quantum dots layers together [19]. However, no detailed simulation studies of surface hexagonal nanoconical frustum arrays based solar cells have been reported.

In this letter, silicon square nanoconical hole (SiSNH) arrays with high aspect ratio and a variety of geometries are introduced for texturing silicon film, the optical properties and energy density distribution of the light field of the proposed nanostructure are theoretically studied via simulation based on Rigorous Coupled Wave Analysis (RCWA) and Finite Difference Time Domain (FDTD) in detail. We found significant enhancements in absorption and enhanced conversion efficiency of silicon solar cells with SiSNH arrays. When the parameters D_{bot}, D_{top} (equal to P), film thickness (H) and hole depth (L) are fixed to be 100, 700, 800 and 1000 nm respectively, solar cells with surface textured SiSNH arrays can yield an photoelectric conversion efficiency of 38.48%. This value is 2.78 times of a 2.33 μm thick Si thin film solar cells. Furthermore, the enhanced conversion efficiency is insensitive to D_{bot}, which would facilitate SiSNH arrays surface texturing in solar cells applications. The possible physics mechanism behind the observation is also explored in this paper.

2. Principle and numerical modeling

The core algorithms based on RCWA [23] and FDTD [24] in this paper are used to find the solution of Maxwell's equations for the light propagation in the trapping structure. RCWA represents the electromagnetic fields as a sum over coupled waves. A periodic permittivity function is represented using Fourier harmonics. Each coupled wave is related to a Fourier harmonic, allowing the full vectorial Maxwell's equations to be solved in the Fourier domain. Then the diffraction efficiency are calculated at the end of simulation. The spatial field distributions are derived from the Fourier harmonics. In order to calculate accurately diffraction efficiencies for all diffraction orders, fine simulation grids are essential, but the key lies in the value of the harmonic wave number, the greater the number of harmonics used, the more accurate the simulation will be. However, this will result in an increased simulation time. While using more harmonics will result in a more accurate index representation, it is not always necessary. Therefore, the best way to determine whether the harmonic number is sufficient for a desired accuracy is to study the convergence of the calculation. In this paper, a convergence study is performed to determine if enough harmonics are being used before our simulation, as shown in the following Table 1.

Table 1. Reflection and absorption of the representative sample (with the parameters D_{top} (equal to P), D_{bot}, H and L take the values of 700 nm, 100 nm, 800 nm and 1000 nm, respectively) under grid size with x nm×y nm×z nm=1 nm×1nm×1 nm and normal incident light (718.5 nm) with different harmonics/(x×y).

Harmonics	2×2	3×3	4×4	5×5	6×6	7×7	8×8	9×9
Reflection	1.26E-001	3.32E-001	1.30E-001	1.23E-001	8.74E-002	6.97E-002	6.03E-002	7.47E-002
Absorption	7.97E-001	6.61E-001	8.67E-001	8.71E-001	9.03E-001	9.18E-001	9.27E-001	9.12E-001

We find that the calculated diffraction efficiencies converge to the stable value with an increasing number of space harmonics. In addition, the convergence study of 2.33 μm thick Si film was also calculated with the same harmonics like Table above (not shown), but calculated diffraction efficiencies of the 2.33 μm thick Si film were unchangeable with different harmonics. The results show that low harmonics are enough for accurate diffraction efficiencies of the 2.33 μm thick Si film, and more harmonics are required for the proposed nanostructure. In order to save simulation time and calculation cost, and to achieve more accurate diffraction efficiency, finally, the fine grid (1 nm×1 nm×1 nm) and the harmonics (8×8, in x and y direction) were adopted in the following simulation for ensuring the convergence and accuracy. The reflection (R) and transmission (T) of a structure can be obtained by decomposing the fields into plane wave components based on RCWA method. According to energy conservation, the

optical absorption of the proposed surface texture is given by A=1-R-T, which is realized by using the periodic boundary conditions in x and y direction to extend infinitely the structural unit (shown in Fig. 1(b)), as shown in Fig. 1(a).

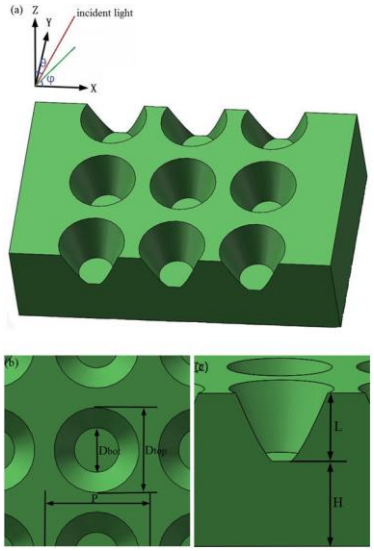

Fig.1. (a) Schematic drawing of 3D SiSNH arrays. (b) 2D top view of 3D SiSNH arrays. (c) Side view of 3D SiSNH arrays

The direction of the incident light is determined by the zenith angle (θ) and azimuthal angle (φ). In the following simulation experiment, both zenith and azimuthal angles are fixed to be zero unless otherwise stated. Therefore, the incident light propagates along the Z axis and the polarization direction is parallel to the X axis, and the incident light energy varies from 1.1 ev to 4 ev. Fig. 1(a) shows the schematic of the proposed SiSNH arrays textured in the surface of Si film solar cells. The SiSNH arrays located at the top part of the underlying structure and are arranged along the XY plane. The parameters of the proposed structure have the period (P) of the hexagonal lattice, the top diameter (D_{top}), the bottom diameter (D_{bot}) and the length (L, equal to the sum of hole depth and film thickness H) of SiSNH arrays, as shown in Fig. 1(b) and (c). The thickness (H) of the underlying Si film in SiSNH arrays is fixed to be 800 nm along the z direction. The refractive index (n) and the absorption index (k) of the crystalline silicon are taken as that in Ref. [25]. We assume that c-Si here are doped lightly, so that both n-type and p-type regions can be modeled using the same refractive n and the same absorption index k as intrinsic crystalline silicon.

In order to quantify the light trapping capability of the proposed surface texture over the solar spectrum, the photoelectric conversion efficiency [26] is calculated according to the following Eq. (1):

$$\eta = \frac{\int_{E_g}^{4.00} E_g I(E) A(E)/E \, dE}{\int_{0.31}^{4.00} I(E) dE} \quad (1)$$

where, Eg=1.1 ev is the band gap of c-Si, E expresses photon energy, I(E) expresses the solar energy density spectrum of ASTM (air mass 1.5 direct normal and circum solar spectrum) [27], and A(E) is the absorption spectrum of the surface texture. Eq.(1) assumed that all the photons with the energy higher than Eg, which can be trapped by the proposed surface texture, would be converted into excitons with the energy of Eg, which means that it doesn't consider the annihilation between the photon and the electron. The excessive energy is converted into heat, and all the photo-generated carriers can be completely extracted for electrical output. The carrier recombination processes within the light trapping structure are not taken into account. In other words, the internal quantum efficiency is assumed to be 100%.

3. Results and discussion

Fig. 2(a)-(c) display the absorption, reflection and transmission spectra of the proposed light trapping structure with different D_{top}, the parameters D_{bot}, period P, film thickness H and hole depth L are fixed to be 100, 700, 800 and 1000 nm, respectively. There are two remarkable trends in the absorption spectra with an increase in D_{top} as shown in Fig. 2(a). (1) The light trapping capability in the high energy region (above 2.2 ev) enhances with the increase of D_{top}, which is consistent with the previous report [3] but different from that in Ref. [2]. (2) The absorption edge shifts towards the low energy end with the increase of D_{top}. It is worth noting that many narrow and irregularly cavity-resonance and guided-spaced resonance peaks appear in the low region, which is different from Fabry-Perot-type resonances by reflections off the top and bottom interfaces in the 2.33 μm thick Si thin film. The significantly enhanced light absorption in the high energy region stems from the surface antireflection of SiSNH arrays, which is due to strong absorption coefficients and the formed graded refractive index of the light trapping structure. In the low energy region, the absorption edge redshifts owning to the cavity-resonance and guided-spaced resonance peaks induced by diffraction between incident light and SiSNH arrays [7].

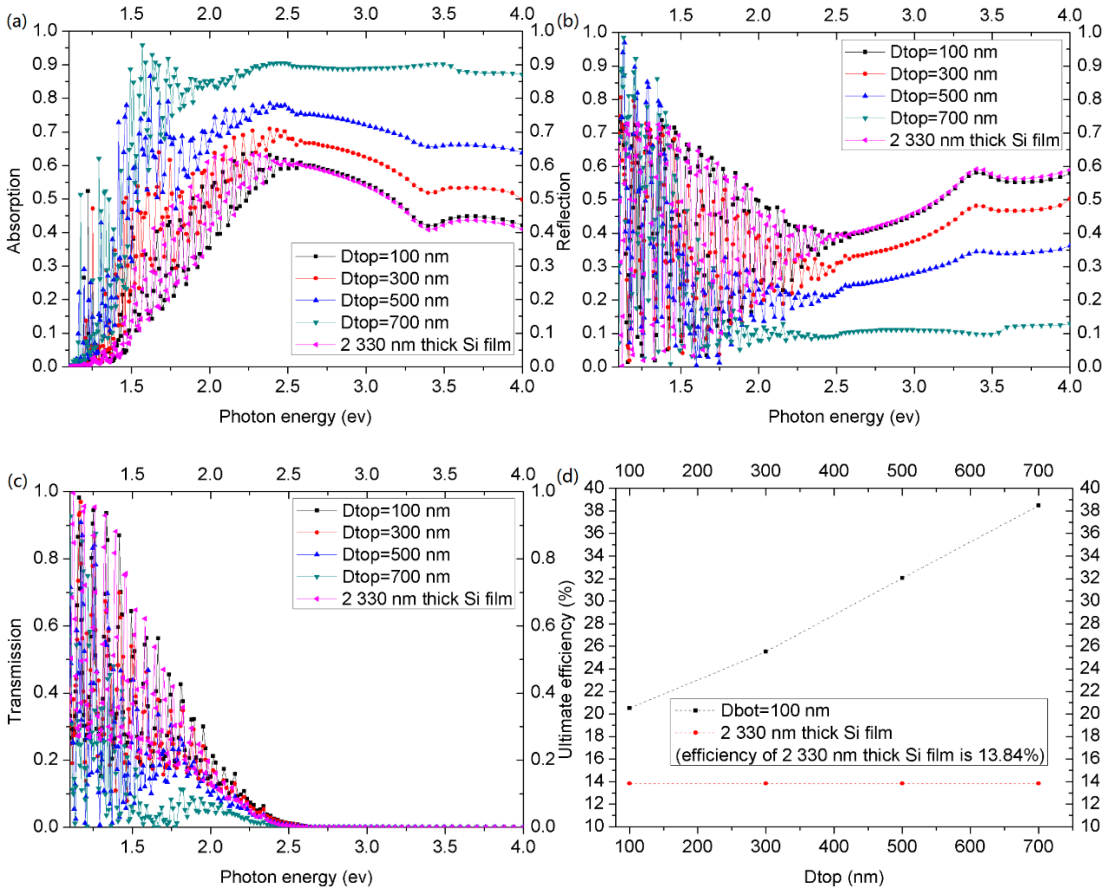

Fig. 2. (a) Absorption, (b) reflection and (c) transmission spectra of the proposed SiSNH structure as a function of D_{top}, the parameters D_{bot}, P, H and L are fixed to be 100, 700, 800 and 1000 nm, respectively. The ultimate efficiency is summarized in (d), the 2.33 μm thick Si film serves as the reference

An ultimate efficiency (13.84%) for the 2.33 μm thick Si film solar cells structure based on the absorption spectra of Fig. 2(a) is quite consistent with the value (13.83%) in Ref. [28]. Fig. 2(d) shows the ultimate efficiency as a function of D_{top} with a fixed D_{bot} (100 nm) and takes 2.33 μm thick Si film solar cells as a reference. It is easy to find that the ultimate efficiency is greatly enhanced. The ultimate efficiency increases with the increasing of D_{top}, and this is consistent with the absorption spectra shown in Fig. 2(a). It is worth noting that an ultimate efficiency of 38.48%, about 2.78 times higher than that of 2.33 μm thick Si film, could be obtained when D_{top} takes the same value as P. This demonstrates that this SiSNH arrays coated Si films has an important potential applications in solar cells. Consequently, the D_{top} (equal to P) is adopted as the optimized value in the following studies.

To understand the trend of absorption in the film solar cells textured by SiSNH arrays, Fig. 3(a)-(c) display the absorption, reflectance and transmittance spectra of our representative structures and take the 2.33 μm thick Si film as a reference. One can find that the absorption spectra of the studied structure with D_{top} (equal to P, 300 nm) displays Fabry-Perot-type resonances as that of the 2.33 μm thick Si film in the low energy region (below 2.5 ev), while the absorption value is higher than that of the 2.33 μm thick Si film in the high energy. Comparing with thin films, the proposed structures have strong absorption in a wide spectrum range when D_{top} (equal to P) takes the value of higher than 500 nm. In the low energy region (above 2.2 ev), the absorption value is near 0.90. In addition, narrow and irregularly cavity-resonance and guided-resonance peaks enhanced the absorption in the low region until the P reach to 700 nm, and the absorption peaks degrade slowly with further increasing of P.

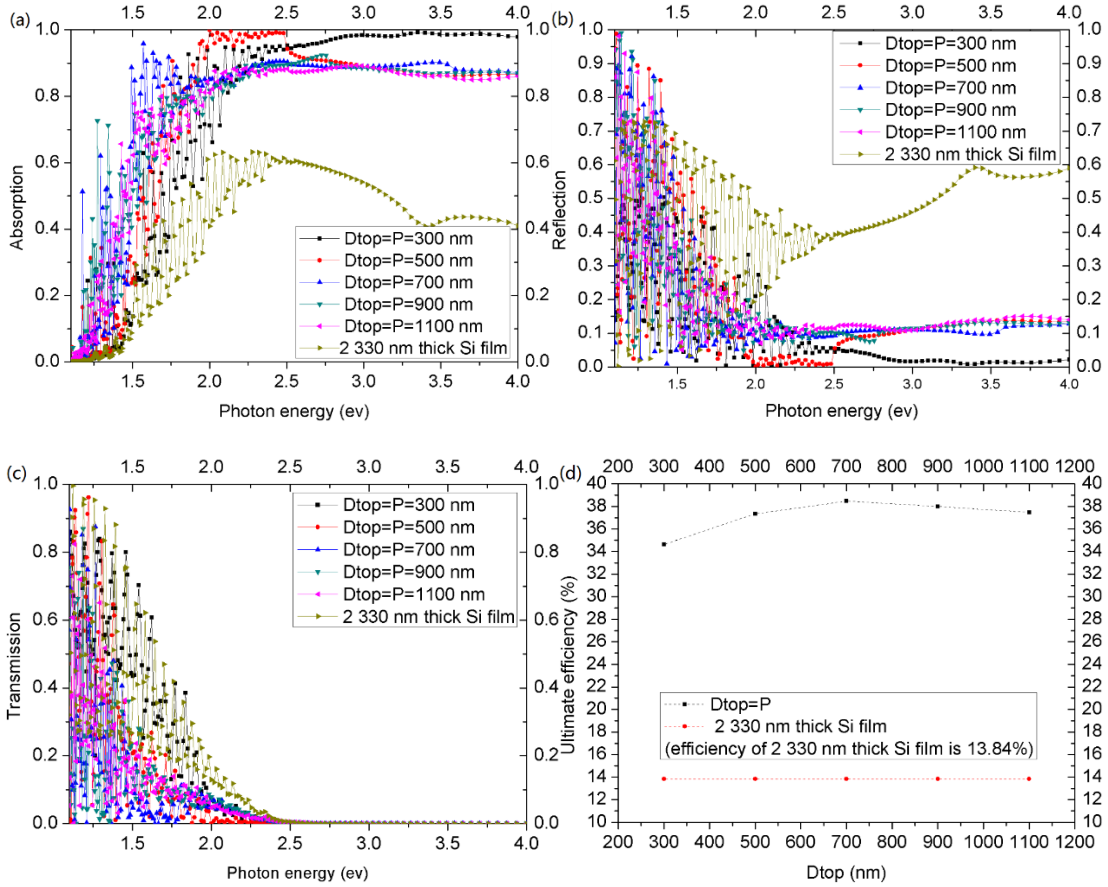

Fig. 3. (a) Absorption, (b) reflection and (c) transmission spectra of the studied SiSNH structure as a function of D_{top}=P, the parameters D_{bot}, H and L are fixed to be 100, 800 and 1000 nm, respectively. The ultimate efficiency is summarized in (d), the 2.33 μm thick Si film serves as the reference

For periodic structures, cavity-resonances and guided resonances stem from the coupling of normally incident light to a superposition of modes propagating in the plane of the arrays. This mechanism enhances light trapping of SiSNH arrays and thus increases the optical absorption. The absorption spectra exhibits more guided resonance enhancement peaks with the increasing of the top diameter D_{top} (equal to P). However, the guided resonance peaks can only emerge at frequencies within the solar spectrum when the lattice constant (P) is sufficiently large [29]. In the high energy region, when the top diameter D_{top} (equal to P) takes the smaller value, such as 300 nm for this structure, antireflection of the front surface of the array structure dominates the absorption enhancement behavior due to stronger absorption capability of the surface texture and the graded refractive index between air and crystalline Si thin film. In the low energy range, high-order diffraction cut-off is the main reason for leading to lower absorption enhancement and the lower ultimate conversion efficiency. For the top diameter D_{top} (equal to P) with the value of 1100 nm, the absorption peaks degrade in the low energy region due to the high reflection loss and mode leakage. Higher ultimate efficiency is achieved when the top diameter D_{top} (equal to P) takes the value of 700 nm, due to the good antireflection performance, cavity-resonances and guide-resonances excitation in the absorption spectra over broadband and broad height range [7].

The absorption spectra of the studied SiSNH structure have a great enhancement in the range from about 2.0 ev to about 2.5 ev for D_{top}=P=500 nm in Fig. 3(a). To illustrate the problem more visually, we also calculate the absorption spectra of various structures, as shown in the following Fig. 4.

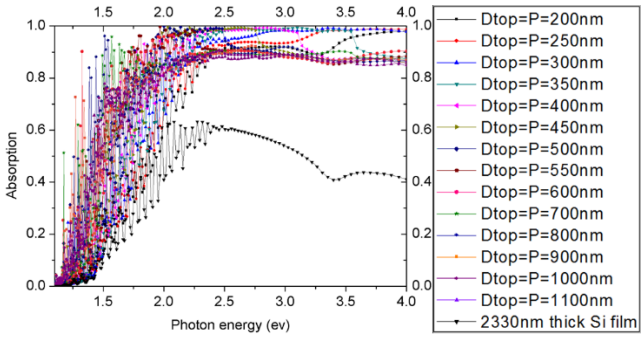

Fig. 4. Absorption spectra of the studied SiSNH structure as a function of D_{top}=P, the parameters D_{bot}, H and L are fixed to be 100, 800 and 1000 nm, respectively. The 2.33 μm thick Si film serves as the reference

Among them in the above absorption spectra, some of the spectra are strongly absorbed, as shown in the following Fig. 5.

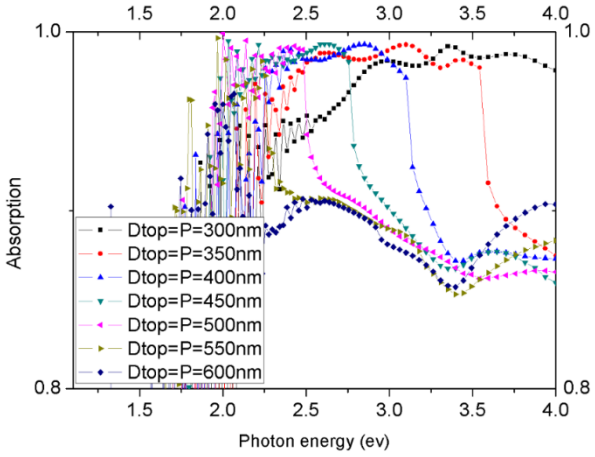

Fig. 5. The absorption spectra of the studied SiSNH structure have a great enhancement for D_{top}= P = 350 nm, 400 nm, 450 nm, 500 nm, 550 nm within the Fig. 4

According to Fig. 4 and Fig. 5, we can find that the absorption spectra of the studied SiSNH structure have also a great enhancement for D_{top}=P=350 nm, 400 nm, 450 nm, 500 nm, 550 nm.

The phenomenon mainly result from the following reasons.

Note that the absorption spectra of the studied SiSNH structure owns Fabry-Perot-type resonances as that of the 2.33 μm thick Si film in the low energy region of 1.5 ev-2.5 ev (for D_{top}=P=350 nm) [30-32] in Fig.4 and Fig.5, while in the high energy the absorption is significantly enhanced. In addition, with the increase of D_{top}, the absorption edge significantly shifts toward the low energy region, which is attributed to irregularly cavity resonances and guided mode resonances enhancement peaks [30]. In the high energy region, antireflection of their front surface dominates the absorption enhancement behavior due to their stronger absorption coefficients and the graded refractive index between air and Si thin film [30-32], and there is a cut-off frequency of the strong absorption. According to the diffraction law and the formula for calculating photon energy, we can obtain the photon energy (E) corresponding with the cut-off frequency of the strong absorption. For the structure with D_{top}=P=350 nm, when $\lambda=D_{top}$, E=1240/λ=3.54 ev, this is exactly the same as the photon energy in Fig.5. Similarly, the photon energy (E) corresponding with the cut-off frequency of the strong absorption for the structure with D_{top}=P=400 nm, D_{top}=P=450 nm, D_{top}=P=500 nm, and D_{top}=P=550 nm are 3.1 ev, 2.75 ev, 2.48 ev and 2.25 ev, respectively. These are also exactly the same as the photon energy in Fig.5. Consequently, when the incident light wavelength is close to the barrier size (D_{top}), the absorption enhancement of spectra appears. This phenomenon attribute to Fabry-Perot-type resonances and array diffraction.

In addition, the ultimate efficiency as a function of D_{top} is shown in Fig. 3(d). Note that the ultimate efficiency peak appears when D_{top} (equal to P) takes the value of 700 nm, which is consistent with the variation of the absorption as shown in Fig. 3(a). According to the graph, the film solar cells with the SiSNH arrays surface texturing can achieve an ultimate efficiency of 38.48% when the parameters bottom diameter D_{bot}, top diameter D_{top} (equal to P), film thickness H and hole depth L take the values of 100, 700, 800 and 1000 nm, respectively. In comparison, previous work showed that the optimal Si nanopillar decorated surface based solar cells with 800 nm thick Si film, a periodicity constant of 500 nm only can yield an ultimate photoelectric conversion efficiency of about 27% [2]. It indicates that the SiSNH arrays coated Si films with high aspect ratio is tremendously promising as a candidate for the high-efficiency Si thin film solar cells. Therefore, such structure is taken as the representative model for the further studies.

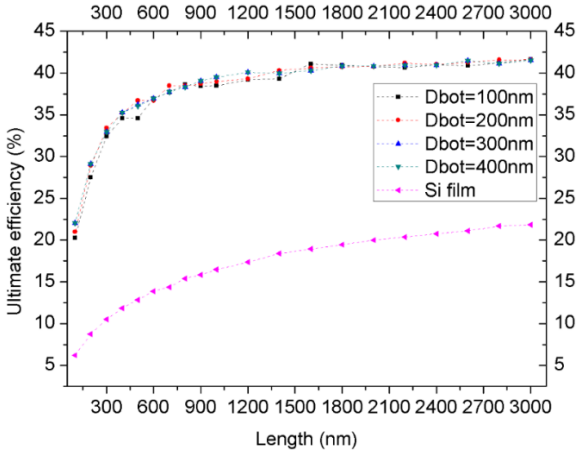

Fig. 6. Ultimate efficiency of the proposed Si solar cells as a function of SiSNH arrays length with different D_{bot}. The Si film with the same thickness of silicon serves as the reference

In order to evaluate the influence of D_{bot}, the parameters D_{top} (equal to P) and film thickness H are fixed to be 700 and 800 nm, respectively, the ultimate efficiency as a function of SiSNH arrays length with different D_{bot} is shown in Fig. 6. Meanwhile, the photoelectric conversion efficiency of Si film solar cells is taken as a reference, we note that the ultimate efficiency of Si film solar cells increases with the increasing of Si film thickness (Length). However, it is still far less than that of the proposed SiSNH arrays with the same thickness of silicon. One can also find that the ultimate efficiency is insensitive to the bottom diameter D_{bot}, which would facilitate the preparation of solar cells with SiSNH arrays

surface texturing. Such observation agrees well with Ref. [14].

Finally, In order to observe visually the effect of SiSNH arrays on the light absorption enhancement, we study the distribution about the electromagnetic field energy density in detail.

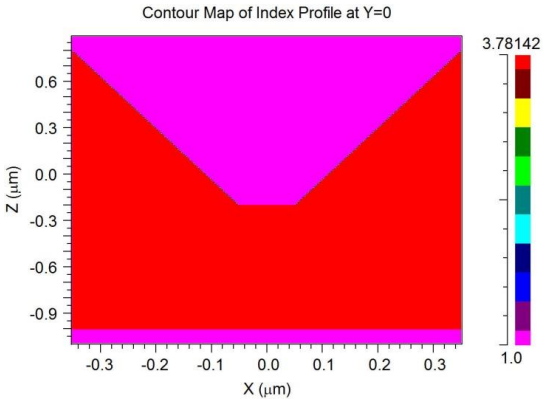

Fig. 7. 2D refractive index distribution of the simulation model in X-Z plane (Y=0) under the normal incident light with 0.7 μm

Under the normal incident light at 0.7 μm, Fig. 7 displays the refractive index distribution of the 3D (three-dimensional) optimizing model (the bottom diameter D_{bot}, top diameter D_{top} (equal to P), film thickness H and hole depth L take the value of 100 nm、700 nm、800 nm and 1000 nm respectively) in X-Z plane(Y=0).

Before calculating the electromagnetic field distribution, it is necessary to calculate the steady-state distribution time of the electromagnetic field via RCWA convergence analysis. According to the Courant stability condition [19] and mesh optimization settings, the time limit step of the stability calculation is 0.0005773502692CT, we employ 0.0005CT as the time step (FDTD_time_step) in the calculation. Under the incident light wavelength at 0.7 μm, we set the different terminal time (FDTD_Stop_Time) to execute the convergence analysis. Here FDTD_Stop_Time=2^n×FDTD_monitor_time=2^n×FDTD_time_step=STn, n=12, 14, 16, 17, that is to say, STn=ST12, ST14, ST16, ST17. According to the following color nephogram (Fig.8) about the energy density distribution, with the extension of the simulation time, the energy density of the electric field E and magnetic field H tend gradually to the steady-state distribution under the different terminal time ST12, ST14, ST16 and ST17. In order to ensure the accuracy of the calculation and save calculation time, we employ ST16 as the terminal time in the subsequent simulation analysis.

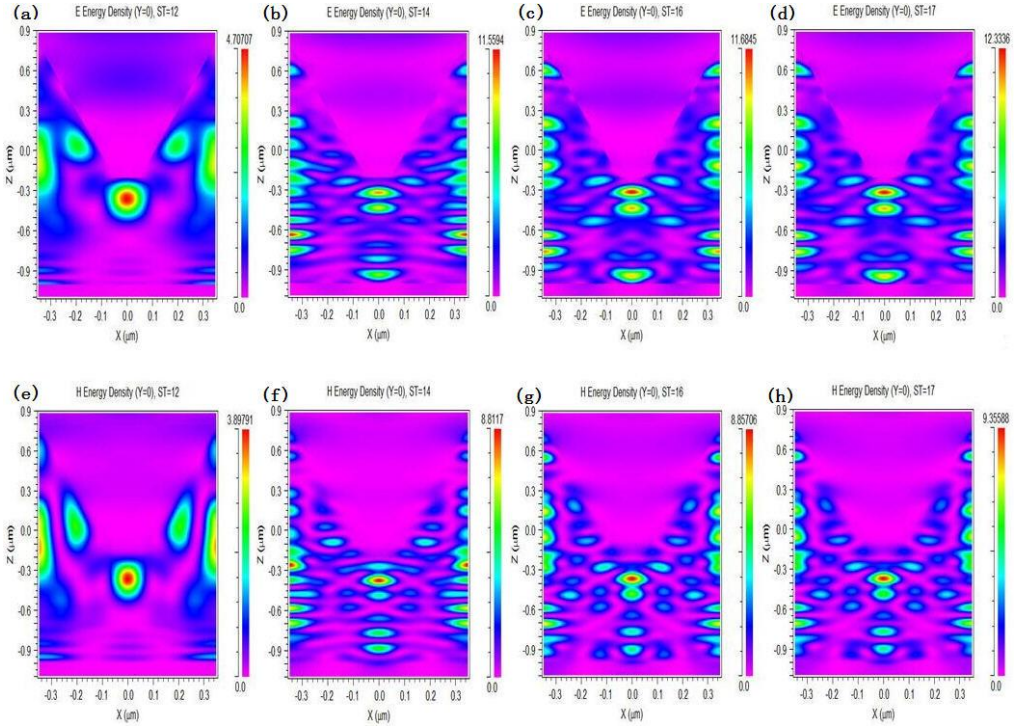

Fig. 8. The E ((a)-(d)) and H((e)-(h)) field energy density distribution of optimized sample with different FDTD_Stop_Time (ST12、ST14、ST16 and ST17) in X-Z plane (Y=0) under normal incident light (0.7 μm)

Under the terminal time ST16 and the different incident light wavelength at 0.35 μm, 0.70 μm and 1.05 μm, Fig. 9 displays the electric and magnetic field energy density distribution of the optimized structure in X-Z plane (Y=0). When the incident light wavelength is 0.35 μm, the incident energy is absorbed by the silicon and attenuated to 1/e of the original energy, the corresponding absorption length is about 9.31×10^{-3} μm [33]. According to Fig. 9(a) and Fig. 9(d), electromagnetic field energy density is mainly distributed among SiSNH arrays structure and the structure surface, that is to say, the incident light is absorbed [14] completely at around 10 nm deep below the surface of the SiSNH arrays structure. According to the absorption spectra in Fig. 3(a), due to larger absorption coefficients [7] of the silicon material and the lower reflection formed by the graded refractive index between air and Si thin film, the spectral absorption value is 98.556% under the incident light wavelength at 0.35 μm (3.54 ev). When the electromagnetic field energy density is simulated with incident light wavelength at 0.70 μm, the incident energy is absorbed by Si and attenuated to 1/e of the original energy, and the corresponding absorption length is about 4.43 μm [33]. As seen from Fig. 9(b) and Fig. 9(e), electromagnetic field is mainly distributed among SiSNH arrays structure, and the spectral absorption value is 52.325% under the incident light wavelength at 0.70 μm (1.78 ev) in Fig. 3(a). This indicates that the incident light wavelength is comparable to the period size of SiSNH arrays structure and then could produce more beams with high diffraction angle, and total reflection will occur when most of beams run into the thin film on the substrate, this will constrain most of beams within the silicon absorption layer, increase the transmission path length of photons, and finally improve the absorption efficiency. When the incident light wavelength is 1.05 μm, the incident energy is absorbed by Si and attenuated to 1/e of the original energy, the corresponding absorption length is about 811 μm, and the spectral absorption value is 0.34% under the incident light wavelength at 1.05 μm (1.18 ev) in Fig. 3(a). As shown in the following diagram Fig. 9(c) and Fig. 9(f), although the energy density of electromagnetic field is stronger, most of beams escape from the silicon absorption layer, thus absorption efficiency of silicon is too low.

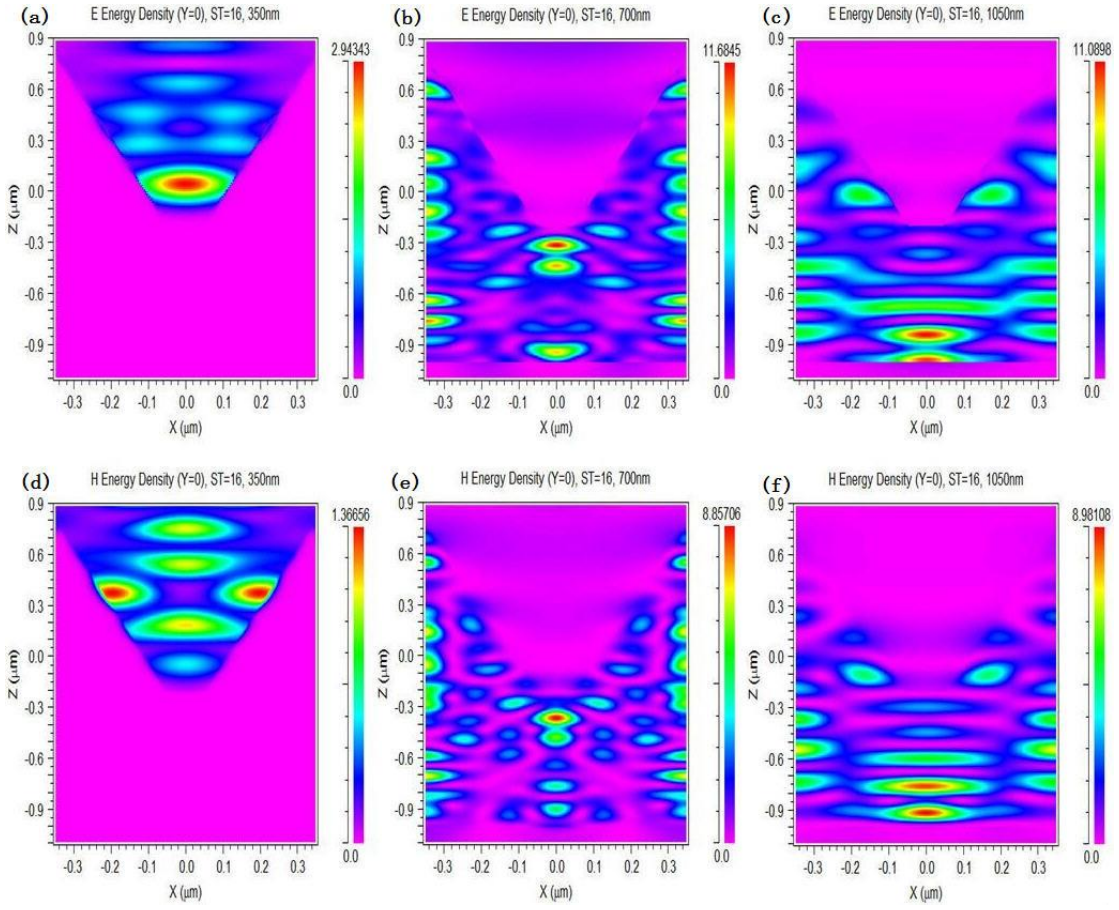

Fig. 9. The electric and magnetic field energy density distribution of the optimized texture with ST16 in X-Z plane (Y=0) under different incident light

4. Conclusions

In summary, we have systematically studied the optical absorption and optical field energy density distribution of light trapping surface textures for photovoltaic applications. Our calculation shows that the incident light absorption of the Si film can be significantly enhanced over broadband and broad height range after preparing SiSNH arrays on Si film surface. It is obtained that the top diameter (D_{top}) of SiSNH arrays should be equal to the array periodicity for efficient solar energy harvesting, and the optimized light absorption could be realized, when the depth of SiSNH arrays reaches 1000 nm with D_{bot} equal to 100 nm. An ultimate efficiency of 38.48% can be finally achieved for this structure when the periodicity and Si film thickness takes 700 nm and 800 nm respectively. Compared to nanopillar and square nanoconical frustum structures, the enhanced ultimate efficiency of SiSNH is less sensitive to the SiSNH bottom diameter D_{bot}. Furthermore, it is meaningful found that the optical field energy density distribution in the light trapping structure array is consistent with the conclusion that the aforementioned array structure could enhance the absorption of the optical wave. We also found that the underlying physical mechanism behind the phenomenon, that is to say, the absorption enhancement of SiSNH arrays is caused by its lower reflectance, cavity resonance and more supported guided-mode resonances. Such excellent characteristic would facilitate the preparation of SiSNH arrays texture on the surface of solar cells.

Acknowledgments

This work was supported by Fundamental Research Funds for the Central Universities (Project No. 2014QNA81) and State Key Development Program of Basic Research of China (State 973 Projects, Grant No. 2014CB046300).

References

[1] M. Pagliaro, R. Ciriminna, G. Palmisano, Chem Sus Chem **1,** 880 (2008).
[2] J. S. Li, H. Y. Yu, S. M. Wong, G. Zhang, X. Sun, P. G. Q. Lo, D. L. Kwong, Applied Physics Letters **95,** 033102 (2009).
[3] J. S. Li, H. Y. Yu, S. M. Wong, G. Zhang, P. G. Q. Lo, D. L. Kwong, Journal of Physics D: Applied Physics **43,** 255101 (2010).
[4] C. Zhang, X. F. Li, A. X. Shang, S. L. Wu, Y. H. Zhan, Z. H. Yang, Nanoscale Research Letters **9,** 481 (2014).
[5] J. S. Li, H. Y. Yu, Y. L. Li, Energy Procedia **8,** 180 (2011).
[6] J. S. Li, H. Yu, Y. Li, F. Wang, M. Yang, S. M. Wong, Applied Physics Letters **98,** 021905 (2011).
[7] R. Y. Zhang, B. Shao, J. R. Dong, J. C. Zhang, H. Yang, Journal of Applied Physics **110,** 113105 (2011).
[8] L. Hong, Rusli, X. C. Wang, H. Y. Zheng, J. X. Wang, H. Wang, H. Y. Yu, Nanotechnology **25,** 415303 (2014)
[9] Y. H. Kuang, M. Di Vece, J. K. Rath , L. van Dijk, R. E. I. Schropp, Reports on Progress in Physics **76,** 106502 (2015)
[10] M. Stuckelberger, Y. Riesen, B. Perruche, M. Despeisse, N. Wyrsch, C. Ballif, Journal of Non-crystalline Solids **358,** 2187 (2015).
[11] T. Kieliba, S. Riepe, W. Warta, Journal of Applied Physics **100,** 063706 (2015).
[12] T. Yamazaki, Y. Uraoka, T. Fuyuki, Japanese Journal of Applied Physics Part 1-Regular Papers Brief Communications & Review Papers **45,** 2441 (2015).
[13] S. W. Boettcher, J. M. Spurgeon, M. C. Putnam, E. L. Warren, D. B. Turner-Evans, M. D. Kelzenberg, J. R. Maiolo, H.A. Atwater, N. S. Lewis, Science **327,** 185 (2010).
[14] B. Wang, P.W. Leu Nanotechnology **23,** 194003 (2012).
[15] A. Zhang, Z. Guo, Y. Tao, W. Wang, X. Mao, G. Fan, K. Zhou, S. Qu, Nanoscale research letters **10,** 214 (2015)
[16] D. Guang, R. Wu, A. Zhang, X. Bao, H. Zhou, F. Shen, Z. Guo, J. Optoelectron. Adv. M. **18,** 618 (2016).
[17] A. Zhang, Z. Guo, Optik-International Journal for Light and Electron Optics **127,** 2861 (2016).
[18] J. Y. Jung, Z. Guo, S. W. Jee, H. D. Um, K. T. Park, H. S. Seo, J. Y. Ji, C. T. Kim, J. H. Lee, Optics Express **18,** 13640 (2010).
[19] H. C. Chen, C. C. Lin, H. W Han, Y. L. Tsai, C. H. Chang, H. W. Wang, M. A .Tsai, H. C. Kuo, P. Yu, Optics Express **19,** A1141 (2011).
[20] H. Park, D. Shin, G. Kang, S. Baek, K. Kim, W. J. Padilla, Advanced Materials **23,** 5796 (2011).
[21] P. C. Tseng, P. Yu, H. C. Chen, Y. L. Tsai, H. W. Han, M. A. Tsai, C. H. Chang, H, C. Kuo, Solar Energy Materials and Solar Cells **95,** 2610 (2011).
[22] M. Yang, H. Yu, X. Sun, J. Li, X. Li, L. Ke, J. Hu, F. Wang, Z. Jiao, Solid State Communications **151,** 127 (2011).
[23] L. C. Andreani, A. Bozzola, P. Kowalczewski, M. Liscidini, Solar Energy Materials and Solar Cells **135,** 78 (2015).
[24] F. Q. Zhang , K. Q. Peng, R. N. Sun, Y. Hu, S. T. Lee, Nanotechnology **26,** 375401 (2015).
[25] http://www.ioffe.ru//SVA/NSM/nk/Silicon/Gif/sicr.gif.

[26] W. Shockley, H. J. Queisser, Journal of Applied Physics **32,** 510 (1961).
[27] Air Mass 1.5 Spectra, American Society for Testing and Materials, http://rredc.nreal.gov/solar/spectra/am1.5/.
[28] C. Lin, M. L. Povinelli, Optics Express **17,** 19371 (2009).
[29] D. Duche, L. Escoubas, J. J. Simon, P. Torchio, W. Vervisch, F. Flory, Applied Physics Letters **92,** 193310 (2008).
[30] B. C. Sturmberg, K. B. Dossou, L. C. Botten, A. A. Asatryan, C. G .Poulton, C. M. deSterke, R. C. McPhedran, Optics Express **19,** A1067 (2011).
[31] P. Wangyang, Q. Wang, K. Hu, X. Shen, Optics Communications **310,** 19 (2014).
[32] K. Hu, E. Ding, P. Wangyang, Q. Wang, J. Nanosci. Nanotechnol. **16,** 6037 (2016).
[33] http://refractiveindex.info/legacy/?group=CRYSTALS&material=Si&option=Palik&wavelength.

*Corresponding author: hukx@cumt.edu.cn, shenzhouwieshi@sjtu.edu.cn